Journal of Power Sources 196 (2011) 9792–9799

Contents lists available at ScienceDirect

Journal of Power Sources

journal homepage: www.elsevier.com/locate/jpowsour

Mitigation of the irreversible capacity and electrolyte decomposition in a $LiNi_{0.5}Mn_{1.5}O_4$/nano-TiO_2 Li-ion battery

Sergio Brutti[a,b,*], Valentina Gentili[b], Priscilla Reale[a], Lorenzo Carbone[a], Stefania Panero[a]

[a] Dipartimento di Chimica, Sapienza Università di Roma, p.le Aldo Moro 5, 00185 Roma, Italy
[b] School of Chemistry, Purdie Building, North Haugh, St. Andrews, Fife KY16 9ST, Scotland, UK

ARTICLE INFO

Article history:
Received 16 June 2011
Received in revised form 1 August 2011
Accepted 3 August 2011
Available online 10 August 2011

Keywords:
Li-ion batteries
TiO_2
$LiNi_{0.5}Mn_{1.5}O_4$
Coating
Irreversible capacity reduction

ABSTRACT

Nanosized titanium oxides can achieve large reversible specific capacity (above 200 mAh g^{-1}) and good rate capabilities, but suffer irreversible capacity losses in the first cycle. Moreover, due to the intrinsic safe operating potential (1.5 V), the use of titanium oxide requires to couple it with high-potential cathodes, such as lithium nickel manganese spinel (LNMO) in order to increase the energy density of the final cell. However the use of the 4.7 V vs. Li^+/Li^0 LNMO cathode material requires to tackle the continuous electrolyte decomposition upon cycling. Coupling these two electrodes to make a lithium ion battery is thus highly appealing but also highly difficult because the cell balancing must account not only for the charge reversibly exchanged by each electrode but also for the irreversible charge losses. In this paper a LNMO-nano TiO_2 Li-ion cell with liquid electrolyte is presented: two innovative approaches on both the cathode and the anode sides were developed in order to mitigate the electrolyte decomposition upon cycling. In particular the LNMO surface was coated with ZnO in order to minimize the surface reactivity, and the TiO_2 nanoparticles where activated by incorporating nano-lithium in the electrode formulation to compensate for the irreversible capacity loss in the first cycle. With these strategies we were able to assemble balanced Li-ion coin cells thus avoiding the use of electrolyte additives and more hazardous and expensive ex-situ SEI preforming chemical or electrochemical procedures.

1. Introduction

Lithium ion batteries are currently employed as power sources for mobile phones, laptops and other portable electronic devices. This market is rapidly expanding due to the worldwide demand. However the transition to new challenging application fields (such as hybrid and electric vehicles, energy storage from intermittent "green" sources) requires to venture beyond the present state of the art by increasing the battery performances and, even more important, by achieving higher safety standards [1,2]. Indeed small scale fires involving Li-ion cells in portable computers have already highlighted the need for a comprehensive understanding and mitigation of the hazard factors [3]. This is even more important when power and energy increase by orders of magnitude in order to run an electric vehicle for hundreds of kilometres [4,5].

Current lithium-ion batteries (LCO-C) comprise of a positive electrode, typically $LiCoO_2$, a negative electrode, typically graphite, and a non-aqueous organic liquid electrolyte. In order to enhance performances and safety possible alternative materials have been intensively studied over the past 15–20 years [2,6,7].

In the standard LCO-C Li-ion cell, safety concerns are mainly related to the use of carbonaceous anodes and carbonate-based electrolytes. Lithium is inserted into graphite (intercalation process) at potentials below 1 V vs. Li^+/Li. At such low potentials, reduction of the electrolyte occurs, accompanied by the formation of a passivation film on the graphite surface. This effect leads to sacrificial charge consumption and dangerous gas evolution in the first insertion process. Moreover most lithium is intercalated into graphite at potentials below 100 mV vs. Li^+/Li^0: again, at such very low potentials, Li could deposit on the anode surface leading to catastrophic dendrite growth and consequential internal short circuiting of the cell. To circumvent the limitation of graphite-based anodes, new alternative materials have been proposed and systematically investigated in the last decade: low-voltage oxides (e.g. titanium oxide-based anodes TiO_2 and $Li_4Ti_5O_{12}$) or metal alloys [6,7]. In both cases "going nano" has been shown to play a critical role. Titanium oxide-based anodes have a double advantage: (a) their working potential falls within the thermodynamic stability window of the standard organic carbonate electrolytes (>0.8 V vs. Li^+/Li^0); (b) they can be easily obtained as nanoparticulates by tuning the synthetic conditions. On the other hand their high operating potential (1.5 V) is also a drawback for energy density. In fact this

* Corresponding author at: Dipartimento di Chimica, Sapienza Università di Roma, p.le Aldo Moro 5, 00185 Roma, Italy. Tel.: +39 06 49913640; fax: +39 0649913951.
E-mail address: sergio.brutti@uniroma1.it (S. Brutti).

0378-7753/$ – see front matter © 2011 Elsevier B.V. All rights reserved.
doi:10.1016/j.jpowsour.2011.08.022

high working potential requires to couple them with high-potential cathodes, e.g. manganese spinel oxides, in order to overcome a simple 2 V LFP-TiO_2 configuration [8,9], thus approaching the performances, in terms of energy density, of a standard $LiCoO_2$-C full cell.

The concept of a 3 V Li-ion cell made by coupling $LiNi_{0.5}Mn_{1.5}O_4$ spinel (LNMO) and TiO_2-based anodes, has been already proposed in the literature in combination with polymer or gel electrolytes [8,10]. However the use of the 4.7 V vs. Li^+/Li^0 lithium nickel manganese spinel cathode material in combination with any lithium electrolyte, requires to address the concomitant increase of parasitic reaction upon cycling. In fact, up to present, no unquestionable solution for stable liquid electrolytes above 4.2–4.5 vs. Li^+/Li^0 has been found yet. This drawback has been proven to be even worse when shifting from a lithium cell configuration to a complete Li-ion cell. In particular, considering a complete LNMO/EC:EMC:$LiPF_6$/Graphite cell, Lee et al. [11] demonstrated the need for tailored electrolyte additives in order to avoid a rapid fade in the reversibly cycled capacity and stabilize the SEI (solid electrolyte interphase) upon cycling. More important, recently, Dedryvere et al. [12] showed that also the "SEI-free" $Li_4Ti_5O_{12}$ anode, in combination with LNMO in a liquid electrolyte, suffers the formation of a composite passivation film of its surface, due to the deposition of large amount of organic and inorganic species at the interface. Therefore practical strategies to passivate the LNMO surface are required for a successful implementation in complete Li-ion cells. Coatings have been proposed in the literature and proven to increase the coulombic efficiency of LNMO upon cycling [13]. In particular oxides precipitated on the surface of LNMO act as HF traps and reduce the Mn dissolution in the electrolyte [13,14].

Turning back on the anode side, in the literature the substitution of the lithium titanate spinel with nano-TiO_2 materials was proposed as the latter can supply a much larger theoretical capacity (i.e. 335 vs. 175 mAh g^{-1} or TiO_2 and $Li_4Ti_5O_{12}$, respectively) [15]. However the adoption of nanomaterials requires to address the additional problem of the enhanced reactivity with the electrolyte and especially the consequent larger irreversible capacity in the first lithium insertion [16]. Typically for graphite, surface pre-treatments, e.g. chemical or electrochemical SEI performing, coatings, fluorination or lithium pre-loading are used to mitigate or compensate the charge loss [17,18]. These strategies are to be preferred to the simple increase of the active mass of the positive electrode in the assembling of balanced Li-ion cell. In fact the latter has a much larger impact on the total mass of the cell and on the specific energy.

In this paper a LNMO-nano TiO_2 Li-ion cell with liquid electrolyte is presented: two innovative approaches on both the cathode- and the anode sides were developed in order to mitigate the electrolyte decomposition, in the first cycle and upon cycling. In particular the LNMO surface was coated with ZnO in order to minimize the surface reactivity upon cycling [19–22]. On the anode side the charge loss in the first cycle suffered by the TiO_2 nanoparticles was compensated by incorporating nano-lithium in the electrode formulation.

2. Experimental details

LNMO was synthesized by co-precipitation from an aqueous solution of the Mn(II), Ni(II) and Li(I) nitrates. Stoichiometric amounts of the precursors nitrates were dissolved in few millilitres of water and the solution was kept at 50 °C under vigorous stirring until complete H_2O evaporation. The mixed nitrate was then transferred in an alumina crucible and fired in air at 800 °C for 12 h. The resulting powder was hand ground and newly annealed at 850 °C for 12 h followed by controlled cooling to room temperature at 1 degree per minute.

The ZnO coating was obtained by suspending the LNMO powder in few millilitres of water by vigorous stirring. A stoichiometric amount of Zn(II) acetate (corresponding to a final ratio of 1.5 wt% of ZnO) was added to the aqueous suspension and the resulting solution was heated and kept under stirring at 40–50 °C for few hours, until complete H_2O evaporation. The resulting composite powder was annealed in air at 500 °C for 30 min with a heating/cooling rate of 1 degree per minute.

The TiO_2 nanoparticulate was commercial anatase nanoparticles AMT-100 (supplied by Tayca Corp., Japan) with nominal crystallite size of 6 nm. The chemical pre-activation of the anode material was obtained by directly incorporating into the electrode mixture nano-lithium powders (Lectro® Max Powder 100, SLMP®, FMC lithium) in fixed ratios. The activated TiO_2 materials were prepared and stored in an argon-filled MBraun glovebox.

The materials were characterized by X-ray diffraction (XRD), scanning electron microscopy (SEM) and transmission electron microscopy (TEM). The XRD experiments were carried out using a Rigaku X-ray Ultima$^+$ diffractometer equipped with a CuKα source and a graphite monochromator for the diffracted beam. The pattern was collected with steps of 0.02 every 9 s. SEM images were obtained by an Oxford Instruments LEO 1450VP. The TEM images were obtained by a JEOL JEM 2011 HR TEM instrument. The electrochemical tests were carried out on pelletized electrodes. The pellets were formed by pressing the composite electrode powder by means of a die set (1.3 mm in diameter) at 6–8 tons. The electrode formulation were for the cathode 80% of the active material (AM), 10% of poly-vinyl-difluoride (PVdF 6020 Solvay Solef) and 10% of SuperP carbon and for the anode 75% of the active material (AM), 10% of poly-vinyl-difluoride (PVdF Kynar) and 15% of SuperP carbon. The electrochemical response of the active materials was tested in coin cells assembled using a working electrode prepared as described above, combined with a lithium counter electrode. The used electrolyte was a 1 M $LiPF_6$ solution in an ethylene carbonate–dimethyl carbonate mixture (LP30), EC:DMC 1:1 (Merck Battery Grade), soaked on a Whatman™ separator. All the manipulations and the cell assemblages were carried out in an MBraun type dry box with moisture and oxygen levels below 1 ppm. The CG tests were carried out at various specific currents, normalized for the active materials weight by using a Maccor Series 4000 Battery Test System.

3. Results and discussion

3.1. Cathode material

The pristine and the ZnO coated LNMO materials show identical XRD patterns (see Fig. 1). In fact at these small ZnO concentration and rather low annealing temperature (500 °C), diffraction is unable to detect the precipitation of zinc oxide, as already pointed out by Sun [19] and Arrebola [22]. In both cases also the expected contamination due to traces of NiO is observed.

The electron microscopy study of the two materials shows well formed sub-micrometric particulates (see Fig. 2). However whereas the SEM analysis does not highlight any difference between the two samples, the TEM micrographs of the ZnO coated material reveal a rough film on the surface of the LNMO crystallites with a thickness of few nanometres. This experimental evidence confirms that the obtained ZnO precipitation forms a coating on the surface of the LNMO sub-micrometric particles rather than clustering in nanoparticles as observed by Arrebola [22]. It is likely that the difference originates from the milder synthesis conditions adopted in this work, similar to those optimized by Sun et al. [19–21] (i.e. very slow precipitation of the zinc acetate precursor on the surface of the LNMO particles, shorter annealing time with moderate heating and cooling rates).

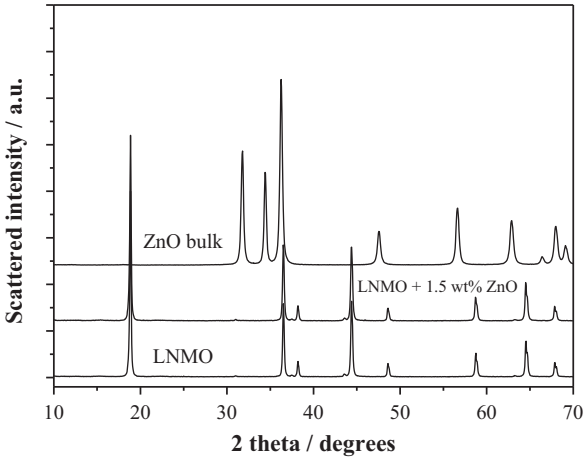

Fig. 1. XRD patterns of LNMO and LNMO coated with ZnO together with the reference spectra of zinc oxide obtained by annealing of zinc acetate at 500 °C.

The two synthesized materials show comparable performances in galvanostatic cycling, as shown in the Fig. 3 at room temperature. The coated material shows increased coulombic efficiencies (for cathodes the ratio between the capacity in discharge and in charge) upon cycling only partially balanced by minor losses in the reversible specific capacity. In particular the coulombic efficiencies of the coated material exceed those of the uncoated material for the firsts 40 cycles at 50 mA g^{-1}. In the following cycles the coulombic efficiencies for both materials are identical within the errors. Moreover the irreversible capacity loss in the first Li de-insertion/insertion of the pristine LNMO is about 35 mAh g^{-1} at 50 mA g^{-1}: this loss is reduced of about 30% in the case of the ZnO coated material. The voltage profiles of the uncoated and coated materials are very similar with a slight increase in the potential hysteresis between charge and discharge for the coated material.

A further analysis of the performances of the two materials cycled at various current rates are presented in Fig. 4. As already observed by Arrebola et al. [22], the specific capacities supplied in the first charge by the uncoated materials are larger compared to the coated material in the entire current range explored. In particular for currents smaller that 100 mA g^{-1} the first charge capacities of the uncoated LNMO exceeded the theoretical value (146.5 mAh g^{-1}). On the contrary in the case of the ZnO coated material, the latter limit is exceeded only for galvanostatic charges at 10 mA g^{-1} (=C/15). In all cases the coulombic efficiency in the first cycle of the coated material is larger compared with the uncoated LNMO at any rates. The two sets of data converge at low currents where an increasing amount of charge is loss also on the coated material.

Besides the reduction of the capacity loss in the first cycle and the increase of the coulombic efficiencies in the first 40 cycles, the capacity retention upon cycling is also improved for the coated material. In fact, for all currents rates, the capacity retention after 10 cycles is larger for the coated material compared with the uncoated.

In summary the reported results confirm that at such high operating voltage vs. Li^+/Li^0 the electrolyte easily undergoes to parasitic oxidations that negatively reflects on the performances

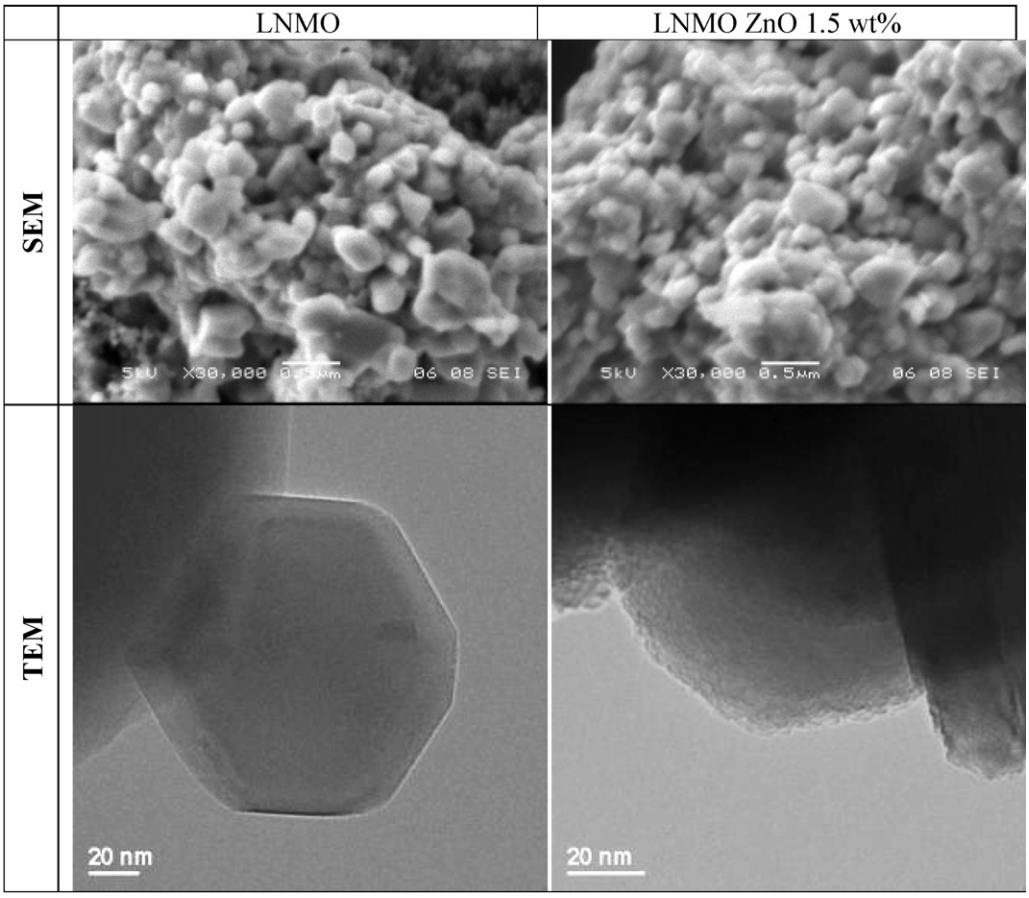

Fig. 2. Electron micrographs of LNMO and LNMO coated with ZnO.

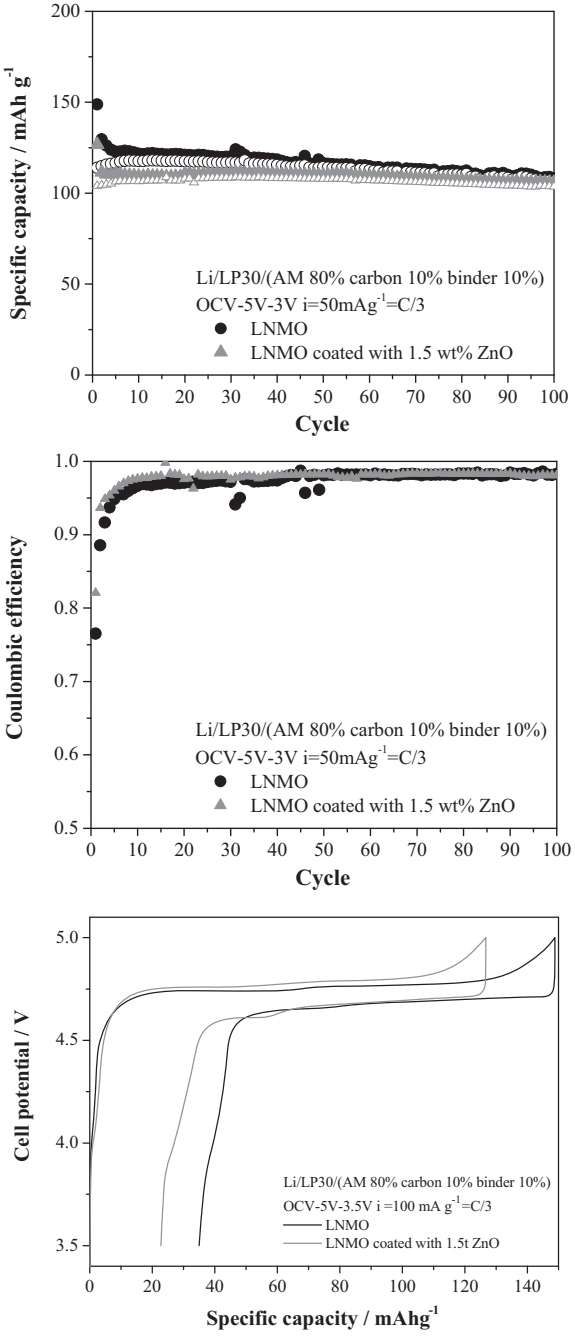

Fig. 3. Galvanostatic cycling of the pristine and the ZnO coated LNMO materials at room temperature (full symbol, charge; hollow symbol, discharge).

of the LNMO material. The passivation of the active material by a ZnO coating partially reduces these drawbacks but at expenses of a slight decrease in the cycled capacity. Briefly the advantages obtained by coating the LNMO surface by ZnO are:

1) A reduced irreversible capacity loss in the first lithium de-insertion/insertion cycle;
2) Larger coulombic efficiencies upon cycling;
3) Improved capacity retention upon cycling.

However, these improvements are partially balanced by the increase in the mean voltage hysteresis between the charge and discharge plateaus. Indeed the sum of the over-potentials in charge and discharge in the galvanostatic voltage profiles rise from 30 mV to 70 mV at 10 mA g^{-1} and 130 mV to 280 mV at 150 mA g^{-1} for the uncoated and coated LNMO, respectively. This larger voltage hysteresis necessarily results in a smaller overall energetic efficiency of the material and requires to be taken into account.

3.2. Anode material

The TiO_2 anode material is formed by anatase nanoparticles. The corresponding XRD diffractogram and transmission electron micrograph are presented in the Fig. 5. The sample is constituted by pure anatase nanocrystals. The nominal particle size of the crystallites was 6 nm. The analysis of the XRD pattern by the Debye–Scherrer equation suggested a slightly larger particle size (10 ± 2) whereas the TEM images suggest a wider interval for the particle size that ranges between 4 and 11 nm.

The cycling of the anatase nanoparticles in a lithium cell is presented in Fig. 6. The material shows a lithium loading in the first cycle that exceeds 0.87 Li atoms per TiO_2 formula unit. This value is much larger than the thermodynamic limit for the lithiation of tetragonal bulk anatase, being the stoichiometry of the lithiated orthorhombic phase $Li_{0.5}TiO_2$. However it has been proven that nanosized anatase particles allow to store more lithium into the structure, by forming the lithium-rich $LiTiO_2$ tetragonal phase [23].

The coulombic efficiency in the first cycle (for anodes it is the ratio between the capacities in charge and discharge) is rather small: only 79% of the charge is reversibly exchanged. This behaviour is not uncommon for nanomaterials and it has been already discussed in the literature for anatase nanoparticles by Wagemaker et al. [16]. In the subsequent cycles the coulombic efficiency increases and it reaches 99% at cycle 14.

In order to mitigate the irreversible capacity loss in the first and in the subsequent cycles, lithium nanopowders were incorporated in the electrode formulation. The coulombic efficiencies and the cycling performances are presented in Fig. 7 for the three composite anode materials containing different amount of lithium, in comparison with the standard electrodes formulation.

The incorporation of lithium in the electrode formulation greatly enhances the reversibility of the electrochemical intercalation/de-intercalation. The coulombic efficiencies in the first cycle increase from 79% of the pristine material to 89%, 100% and 117% for the electrode incorporating 1, 2 and 3 wt% of nano-lithium, respectively.

In order to discuss in more detail the effect of the incorporation of nano-lithium in the electrode formulation, the nominal composition of the electrodes were calculated at the end of the first discharge/charge and summarized in Table 1. Although the 1st discharge Li loadings decrease with the increase of the nano-lithium content in the pristine materials, the overall compositions at the end of discharge, also including the lithium pre-loading, show an increasing trend. On the contrary the overall amount of lithium de-insertion upon charge is constant for all materials and it is therefore not dependent neither on the amount of nano-lithium in the pristine electrodes, nor on the amount of electrochemical lithium insertion upon discharge. In fact the specific capacity supplied in the first charge is about 230 mAh g^{-1} at 100 mA g^{-1} for all the four electrode formulations. This result suggests that this 6 nm anatase nanomaterial is capable to reversibly exchange only 0.7 lithium equivalent per TiO_2 formula unit. As a consequence the nominal amount of lithium kept in the electrode at the end of the first cycle is larger for materials with larger amount of nano-lithium pre-loading. Although a detailed study of the nature of the irreversible capacity in the anatase nanoparticles is beyond the scope of this paper, it is important to recall that irreversible charge losses in lithium cells can be due to either lithium trapping within the hosting crystal lattice of the active material, or surface reactivity with the electrolyte. The latter, in particular, can be initiated by

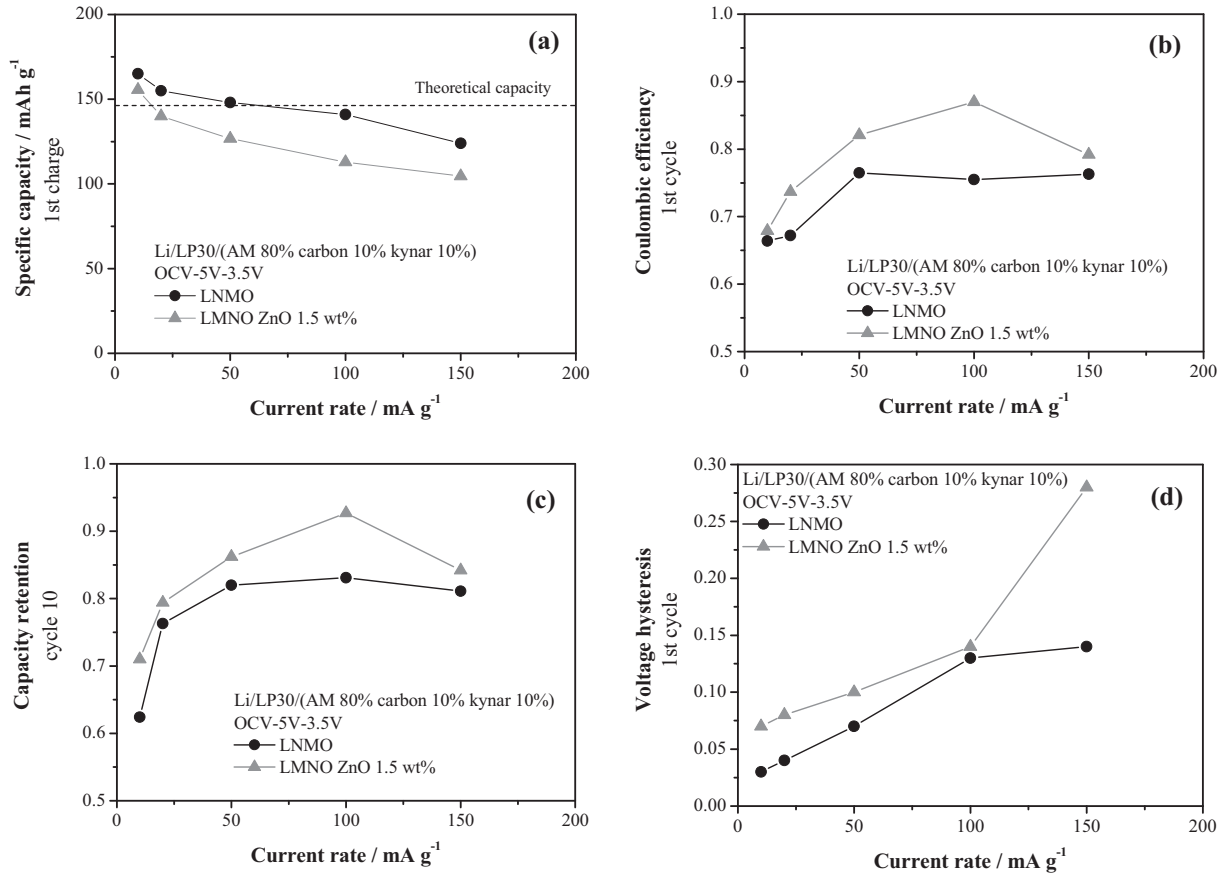

Fig. 4. Comparison of the performances in galvanostatic tests at various current rates for the coated and uncoated materials at room temperature: (a) specific capacities in the first charge/Li de-insertion; (b) coulombic efficiency in the first cycle (i.e. ratio between the specific capacity supplied in the charge and discharge steps in the first cycle); (c) capacity retention at cycle 10 (i.e. ratio between the specific capacity supplied in charge at cycle 10); (d) voltage hysteresis in the first cycle (i.e. mean difference in the voltage plateau for the charge and discharge steps in the first cycle).

the unavoidable OH groups and adsorbed water on the surface of TiO_2 nanostructures [16]. Indeed water traces are known to spontaneously react with the electrolyte components resulting in LiF and complex phosphate species precipitation and HF formation, thus opening the door to further degradation of the electrolyte on reduction [25,26]. In the present study about TiO_2 pre-lithiation in two out of four cases the nominal amount of lithium incorporated in the electrode at the end of discharge overcomes 1 lithium atom per TiO_2 formula unit (see Table 1). It is straightforward that not all the specific capacity can be due to the Ti(IV)/Ti(III) redox couple. It is likely that part of the charge is dissipated in parasitic reactions due to electrolyte decomposition. Unfortunately the present data does not allow further speculations and in particular the decoupling of the two possible origins of the irreversible capacity (lithium trapping vs. electrolyte decomposition). Further work is in progress in our laboratory to tackle this intriguing phenomenon.

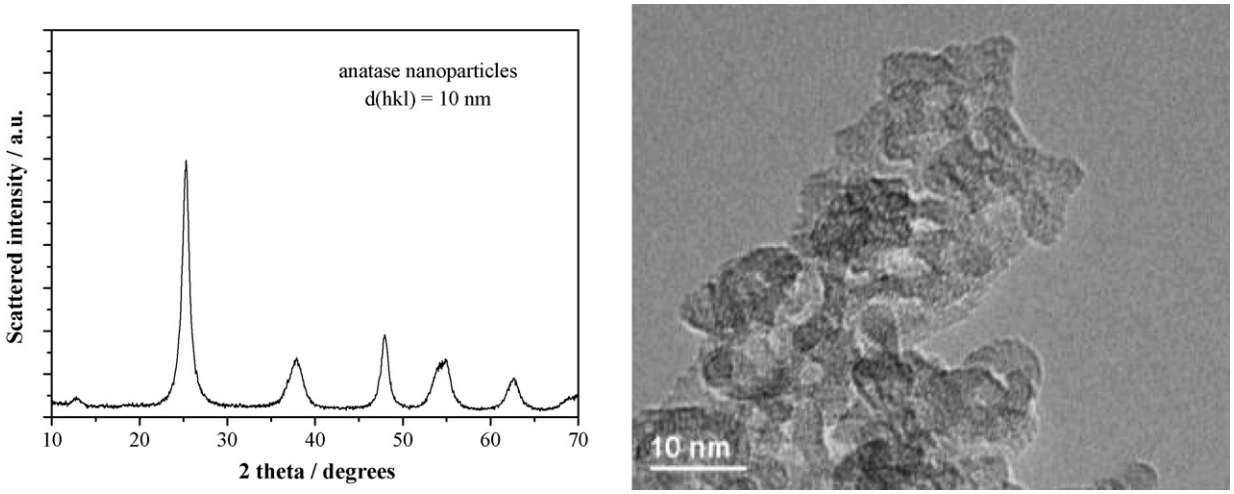

Fig. 5. XRD and transmission electrode microscopy of the anatase nanoparticles.

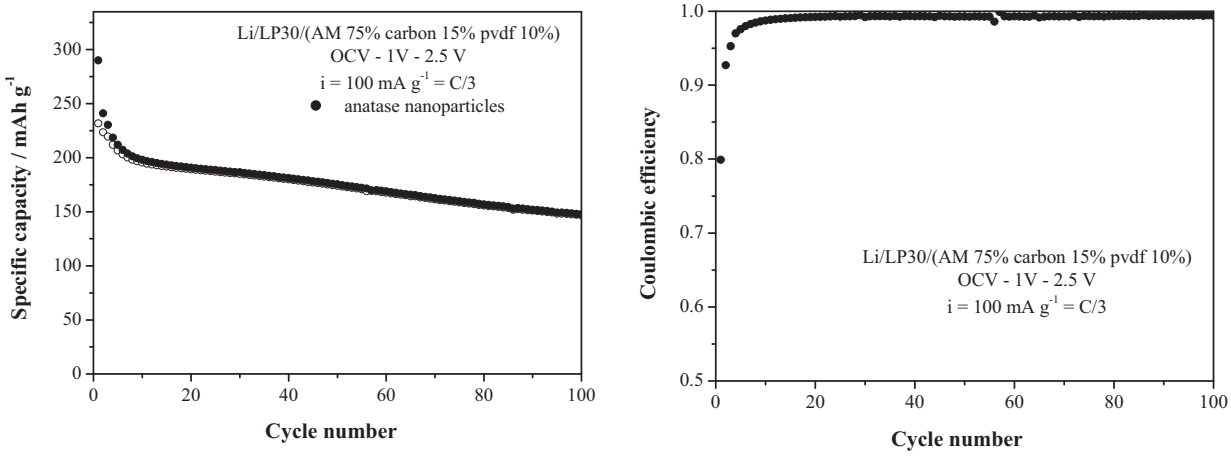

Fig. 6. Galvanostatic cycling of the anatase nanoparticles at room temperature (full symbol, discharge; hollow symbol, charge).

Table 1
Evaluation of the nominal composition of the anatase electrodes pre-activated by incorporating different amounts of nano-lithium (the binder/carbon electrode components are not considered in this evaluation as their amounts have been kept constant; dsch., discharge; ch., charge).

Nano-lithium (wt%)	Nominal pristine composition	Nominal 1st dsch. Li insertion	Nominal composition at the end of 1st dsch.	Nominal 1st ch. Li de-insertion	Nominal composition at the end of the 1st cycle	Coulombic efficiency
0	TiO_2	0.87	$Li_{0.87}TiO_2$	0.68	$Li_{0.19}TiO_2$	0.79
1	$Li_{0.18}TiO_2$	0.77	$Li_{0.95}TiO_2$	0.69	$Li_{0.26}TiO_2$	0.89
2	$Li_{0.36}TiO_2$	0.69	$Li_{1.05}TiO_2$	0.69	$Li_{0.36}TiO_2$	1.00
3	$Li_{0.54}TiO_2$	0.59	$Li_{1.13}TiO_2$	0.68	$Li_{0.45}TiO_2$	1.17

Besides the improvement in the first intercalation/de-intercalation also the further irreversible losses suffered in the first tenth of cycles are greatly decreased. All the three materials containing lithium in the electrode formulation reach a 99% coulombic efficiency at cycle 5. Furthermore the incorporation of lithium does not have negative impact on the reversibly cycled capacity or the capacity retention upon cycling. All the three materials containing lithium are capable to reversibly cycle in lithium cells with performances comparable with those of the pristine anatase nanoparticles. The material containing 2 wt% of nano-lithium appears to be the most suitable for application in complete lithium ion cells as its coulombic efficiency in the first cycle approach 100%.

The voltage profile of this composite electrode is presented in Fig. 8 in comparison with the pristine electrode. The open circuit voltage of the 2% Li composite material is lower, i.e. 1.8–1.75 V, than the standard material, i.e. 2.9–3.0 V. This is probably due to an *in situ* pre-lithiation that occurs when the electrolyte wets the electrode surface. During discharge the lithium loading curve of the composite material starts immediately with the typical voltage plateau due to the tetragonal/orthorhombic two-phase transformation in anatase lithiation [24] without showing any continuous potential change like the pristine material.

Besides the absence of the first potential slope from OCV to the plateau at 1.7 V, the voltage profile of the composite material shows only few minor changes compared with the pristine material: (a) a slight shortening of the voltage plateau at 1.75 V in both discharge/charge, (b) a smoothening of the long discharge tail between 1.7 and 1 V and (c) a slight increase of the over-potentials between discharge and charge. In summary, the incorporation of lithium into the electrode formulation mainly affects the high voltage part of the discharge curve. In this high voltage slope from

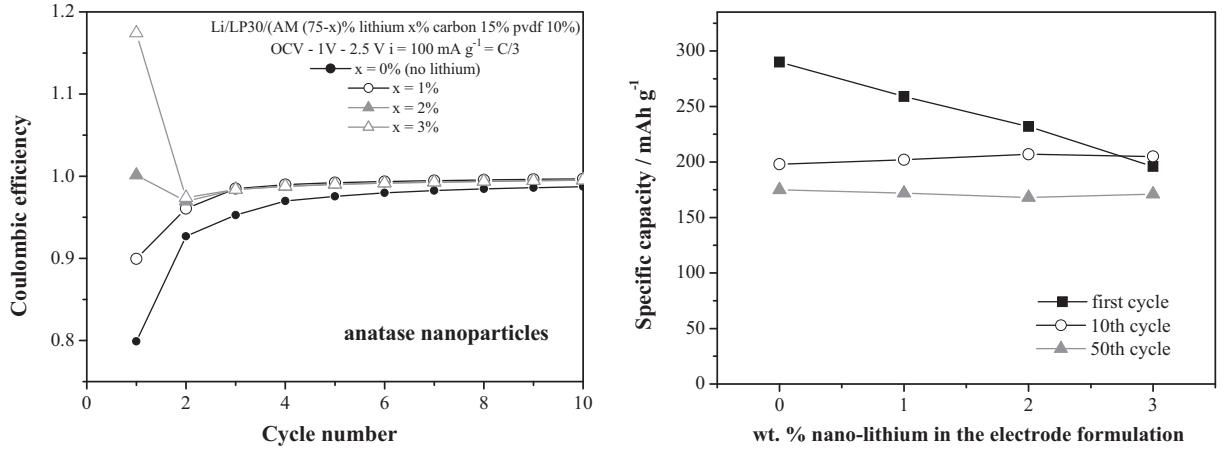

Fig. 7. Coulombic efficiency and capacity retention of the anatase nanoaprticles electrodes containing different amount of nano-Li additive.

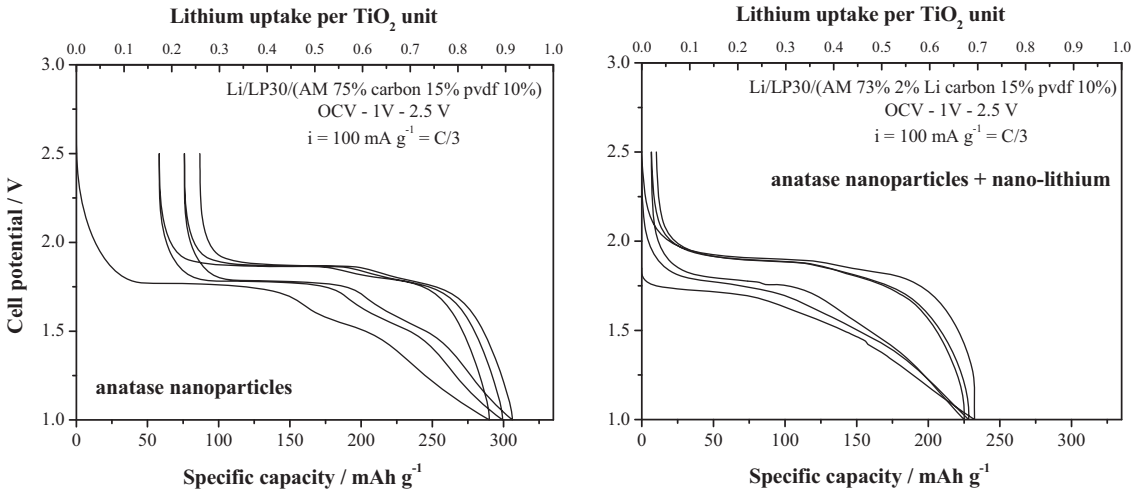

Fig. 8. Voltage profiles of the galvanostatic cycling at 100 mA g^{-1} of the anatase nanopowders wit and without lithium additive in the electrode formulation.

the OCV to the plateau at 1.7 V, the pristine material exchanges 41 mAh g^{-1}: this specific capacity accounts for approximately 70% of the total irreversible capacity loss (i.e. 58 mAh g^{-1}) in the first cycle.

3.3. The Li-ion cell

The rate performances of a complete lithium-ion cell configuration made by coupling the implemented cathode and anode

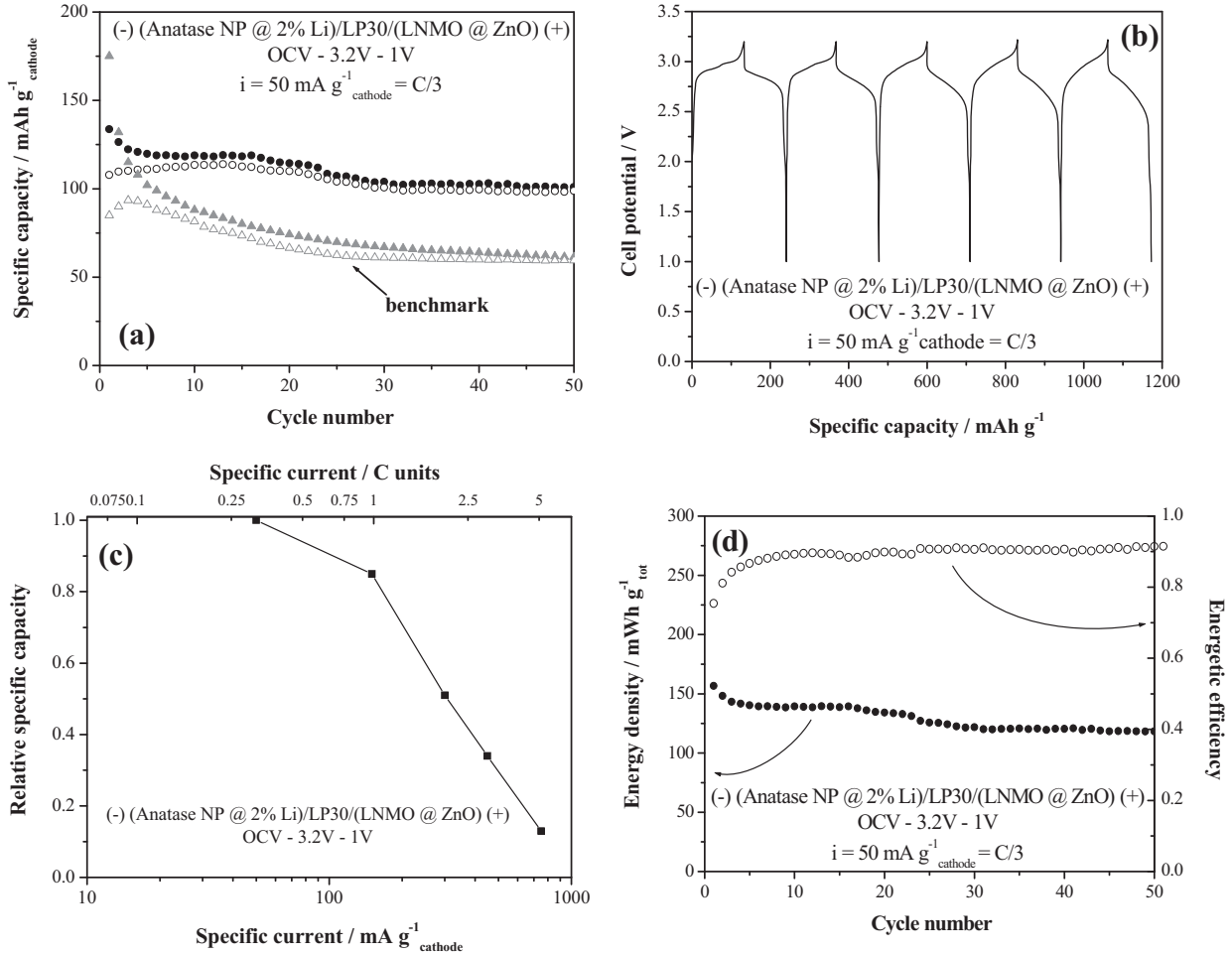

Fig. 9. (a) Specific capacity vs. cycle number, (b) voltage profile, (c) specific capacity vs. current rate and (d) energy density and energetic efficiency of the complete Li-ion cell at room temperature (full symbol, charge; hollow symbol, discharge). The benchmark performances in (a) are referred to a lithium-ion cell assembled with the LNMO and nano-TiO_2 materials without coating and 2% nano-lithium incorporation, respectively.

materials with a LP30 liquid electrolyte are presented in the Fig. 9. This is the first ever reported complete Li-on cell made by nanosized TiO_2 anatase particles with a coated LNMO and a liquid electrolyte. The reported cell is cathode limited as it contains an excess weight of the anode compared to the cathode active material (negative to positive mass ratio N/P = 1.5). The two electrode active materials were not pre-activated electrochemically but simply assembled into a two electrode coin cell configuration and cycled at C/3 (i.e. 50 mA g^{-1}) in respect to the cathode material weight. The corresponding specific current is 0.375 mA cm^{-2}. For the sake of completeness also the performances in the same galvanostatic conditions of a benchmark cell are reported in Fig. 9. The latter has been assembled by using the uncoated LNMO material and the nano-TiO_2 without lithium pre-loading with the same N/P weight ratio.

The coulombic efficiency in the first cycle is 80% and it reaches 95% at cycle 9. The charge loss in the first cycle can be attributed mainly on the residual irreversible capacity of the cathode material (see Fig. 3). The capacity retention is 88% and 75% at cycle 10 and 50, respectively. The mean voltage in charge is 2.93 V and in discharge is 2.78 V. The energy density obtained reaches a stable plateau value around 125 mWh g^{-1} after 30 cycles. The corresponding overall energetic efficiency (i.e. the ratio between the energy density in charge and discharge) approaches 90% after cycle 9.

It is expected that the performances of this cell can be further enhanced by further optimizing the negative to positive electrode mass ratio and by using electrolyte additives as cathode protecting agents (e.g. silanes, LiBOB) or $LiPF_6$ stabilizers (LiF, weak Lewis bases) [27]. Furthermore shifting from nanosized anatase particles to nanostructured particulates (nanorods, nanowires, and nanotubes) is expected to lead to an improvement in the rate capabilities and in the capacity retention. This work is in progress in our laboratory and preliminary results confirm the potential improvements that can be achieved by shifting from nanoparticles to nanostructures.

4. Conclusion

In this paper we presented an innovative formulation for a complete Li-ion cell by coupling a nanosized TiO_2-based anode with a ZnO coated LNMO cathode in a liquid LP30 electrolyte.

The anode and cathode materials have been carefully optimized in order to mitigate the irreversible capacity loss in the first cycle on the anode side, and the parasitic reactions upon cycling on the cathode side. A compact and continuous ZnO coating was precipitated on the surface of the cathode material, whereas the formulation of the anode electrode was optimized by adding nano-lithium powder as pre-lithiating agent.

The resulting Li-ion cell combines the intrinsic superior safety and inherent overcharge protection of TiO_2 compared to graphite, with mitigated liquid electrolyte decomposition on the cathode side provided by the ZnO coating.

In summary the present results demonstrate the potential of anatase nanoparticles and the coated nickel manganese spinel as a valuable combination in future lithium-ion batteries.

Acknowledgments

This research project has been carried out in the frame of the project IIT SEED Realist “Rechargeable, advanced, nanostructured, lithium batteries with high storage capability”. One of the authors (Sergio Brutti) is grateful to the ALISTORE-ERI consortium for the post-doctoral fellowship.

References

[1] J.M. Tarascon, M. Armand, Nature 44 (2001) 359.
[2] M.G. Kim, J. Cho, Adv. Funct. Mater. 19 (1) (2009) 497.
[3] J.S. Gnanaraj, D. Aurbach, J. Power Sources 119–121 (2003) 794.
[4] F.T. Wagner, J. Phys. Chem. Lett. 1 (2010) 2204.
[5] K. Kitoh, H. Nemoto, J. Power Sources 81–82 (1999) 887.
[6] K. Ozawa, Lithium Ion Rechargeable Batteries, Wiley-VCH Weinheim, Germany, 2009.
[7] P.G. Bruce, B. Scrosati, J.M. Tarscon., Angew. Chem. Int. Ed. 47 (2008) 2930.
[8] G. Armstrong, A.R. Armstrong, P.G. Bruce, P. Reale, B. Scrosati., Adv. Mater. 18 (2006) 2597–2600.
[9] F.F. Cao, X-L. Wu, S. Xin, Y-G. Guo, L-J Wan., Phys. Chem. C 114 (2010) 10308–10313.
[10] S. Patoux, L. Daniel, C. Bourbon, H. Lignier, C. Pagano, F. Le Cras, S. Jouanneau, Martinet.F S., J. Power Sources 189 (2009) 344–352.
[11] H. Lee, S. Choi, S. Choi, H-J. Kim, Y. Choi, S. Yoon, J-J Cho, Electrochem. Commun. 9 (2007) 801–806.
[12] R. Dedryvere, D. Foix, S. Franger, S. Patoux, L. Daniel, D. Gonbeau., J. Phys. Chem. C 114 (2010) 10999–11008.
[13] C. Li, H.P. Zhang, L.J. Fu, H. Liu, Y.P. Wua, E. Rahm, R. Holze, H.Q. Wu., Electrochim. Acta 51 (2006) 3872–3883.
[14] H.-B. Kang, S.-T. Myung, K. Amine, S.-M. Lee, Y.-K. Sun, J. Power Sources 195 (2010) 2023–2028.
[15] G. Armstrong, A.R. Armstrong, J. Canales, Bruce.F P.G., Chem. Commun. 245 (2005) 4–2456.
[16] W.J.H. Borghols, D. Lutzenkirchen-Hecht, U. Haake, W. Chan, U. Lafont, E.M. Kelder, E.R.H. van Eck, A.P.M. Kentgens, F. Mulder, M. Wagemaker, J. Electrochem. Soc. 157 (2010) A582–A588.
[17] P. Novak, D. Goers, M.E. Spahr, in: F. Beguin, E. Frackowiak (Eds.), Carbons for Electrochemical Energy Storage and Conversion Systems, CRC Press Inc., USA, 2010, pp. 263–328.
[18] J. Christensen, J. Newman, J. Electrochem. Soc. 152 (2005) A818–A829.
[19] Y.K. Sun, K.J. Hong, J. Prakash, K. Amine., Electrochem. Commun. 4 (2002) 344.
[20] Y.K. Sun, Y.S. Lee, M. Yoshio, K. Amine., Electrochem. Solid State Lett. 5 (2002) A99.
[21] Y.K. Sun, C.S. Yoon, I.H. Oh, Electrochim. Acta 48 (2003) 503.
[22] J.C. Arrebola, A. Caballero, L. Hernan, J. Morales, J. Power Sources 195 (2010) 4278.
[23] M. Wagemaker, W.J.H. Borghols, F.M. Mulder, J. Am. Chem. Soc. 129 (2007) 4323–4327.
[24] Y. Ren, L.J. Hardwick, P.G. Bruce, Angew. Chem. Int. Ed. 49 (2010) 2570–2574.
[25] H. Ota, A. Kominato, W-J. Chun, E. Yasukawa, S. Kasuya, J. Power Sources 119–121 (2003) 393–398.
[26] L. Gireaud, S. Grugeon, S. Pilard, P. Guenot, J.-M. Tarascon, S. Laruelle, Anal. Chem. 78 (2006) 3688–3698.
[27] S.S. Zhang, J. Power Sources 162 (2006) 1379–1394.